EFFECT OF FREE STREAM TURBULENCE ON THE LOADS EXPERIENCED BY AN SG6043 HYDROFOIL

Ashwin Vinod, Angela Lawrence and Arindam Banerjee[1]
Department of Mechanical Engineering and Mechanics
Lehigh University
Bethlehem PA 18015
[1]Corresponding author: arb612@lehigh.edu

INTRODUCTION

Flows occurring in nature are mostly turbulent. Turbulence intensities estimated at some of the potential deployment sites for marine hydrokinetic energy systems range between 6–24%[1]. Such free-stream (inflow) conditions are capable of impacting both performance and structural integrity of the hydrofoils as well as other turbine components; thereby affecting the operational life of these devices.

Free stream turbulence (FST) is the background level of random, three-dimensional velocity fluctuation that is present in a fluid stream. FST at a given location is often characterized by the turbulence intensity and its spectral composition[2, 3]. A large volume of the available literature that deals with various aspects of very complex flows around both aerodynamic and bluff bodies [3-5] are conducted in wind or water tunnels with low levels of FST. Owing to its practical importance, researchers have developed various mechanisms/designs capable of imparting turbulence into flows in a laboratory environment. Such devices called turbulence generators can be primarily classified into two types: (1) Passive Generators and (2) Dynamic Generators. Gad-el-Hak & Corrsin[6] defined a dynamic generator as one that has moving boundaries or adds a mean momentum to a turbulent flow. Any design that does not comply with the above definition is considered a passive generator. A type of dynamic generator, commonly referred to as the active grid was developed by Makita[7, 8] and coworkers at the Toyohashi University of Technology in Japan in the early 80's for use in their wind tunnel, in which agitator winglets are attached to rotating rods creating time varying solidity. This facilitated the production of large scale, high intensity turbulent flow in small low speed facilities not achievable using other kinds of turbulence generators. The Makita design featured 15 rotating horizontal and vertical shafts and they documented turbulence intensities as high as 16%.

Previous studies with the active grid type turbulence generators have used various combinations of operating parameters/forcing protocols to define the dynamic behavior of the system. The three major protocols used most commonly by researchers [7, 9-11] are, synchronous (SN), single random (SR) and double random (DR). The SN protocol is the simplest; in this mode, each winglet shaft rotates at a constant angular velocity for the duration of the test. It allows the user to choose the rotational direction and speed of each winglet shaft. When compared to other protocols, the SN protocol produces smaller turbulence levels, poor lateral homogeneity, slower downstream decay of turbulence energy and the turbulence properties are found to be highly correlated to the initial positions. Also, Makita & Miyamoto[8], Mydlarski & Warhaft[10] and Poorte[11] reported distinctive spikes in the energy spectrum in the lower frequency range, which was caused by the large periodicities in the generated turbulence due to the periodic grid rotation. The SR protocol attempts to excite the lower frequencies in the spectrum uniformly by keeping the angular velocity constant, while switching the direction of rotation of the winglet shafts at random intervals. The time traveled without a change in rotational direction or speed, called the cruise time, is varied randomly between a predetermined minimum and maximum value. Increased turbulence intensity and lateral homogeneity have been reported with the single random protocol. The peaks in the lower frequency region of the energy spectrum are still observed, however with a lower magnitude[10]. The DR Protocol introduced by Poorte[11], randomizes all the three parameters: cruise time, rotational speed and direction. Poorte found that he could change the macro structure of turbulence through the resulting integral time scale by choosing speed and cruise time. The spike in energy spectrum observed with the other protocols was not observed using the double random

profile and the obtained turbulence intensities and isotropy was high.

The current work employs an active grid turbulence generator to systematically analyze the effect of FST on the loads acting on a hydrofoil. The SG6043 hydrofoil was chosen based on its ability to produce high lift forces in the range $10^5<Re<10^6$.[12, 13]. The present study is conducted at a Reynolds number of 1.1×10^5, which is lower than the operating Reynolds numbers of large, industrial scale turbine systems. However, from a mechanistic perspective, such controlled investigations could prove beneficial in untangling the flow physics behind such fluid structure interaction problems. To the knowledge of the authors, this is the first attempt at employing an active grid in a horizontal test section water tunnel to study the effect of FST on loading characteristics of hydrofoils. Previous investigations were mostly performed in wind tunnels and employed passive turbulence generators [14]. The submitted abstract present's results obtained during the preliminary testing of the active grid and the effect of turbulence intensity on the performance of the hydrofoil. An elaborate study discussing the effects of various other aspects of the turbulence generated on the performance of the hydrofoil will be the subject of a follow-up journal publication.

METHODS

All experiments were performed in the open surface recirculating water channel at Lehigh University. Its test section is 24" wide, 24" tall and 78" long and is capable of attaining flow speeds as high as 1m/s. The turbulence generator developed (see figure 1) is a Makita type [7, 8] active grid. It is constituted of ten rotating winglet shafts, with five oriented horizontally and five vertically. The module is 6" long and has an inner cross section of 24" X 24" that mates precisely with the test section entrance of the water channel. This resulted in a mesh size (M) of 4". The 3/8" diameter winglet shafts have six winglets each. The 2.45" side, square winglets are made out of 0.1875" stainless steel sheets and are fastened to the shafts with their diagonals along the axis of the shaft, in a diamond fashion. The shafts are arranged in a bi-planar configuration with all the vertical shafts in one plane and all the horizontal shafts in another, spaced 0.5" apart from each other and symmetric about the center of the active grid module. Each winglet shaft is controlled by a 23 NEMA series, Anaheim Automation 23MDSI stepper motor which includes an onboard simple controller/indexer and a micro-stepping driver. It runs off a 12-24VDC supply with a max power intake of 40W and is capable of generating up to 230oz-in of torque. They use the RS485 communication protocol and accept commands at a baud rate of 38400. In our experiments, the motors are operated at 1600 steps/revolution giving a resolution of 0.225°. In addition to the 60 rotating winglets, the grid is also fitted with 24 fixed, half winglets, upstream of the plane of the rotating winglets, along the inner perimeter of the active grid frame. In order to ensure the absence of water leakage and minimum shaft friction, PTFE V-ring seals are used at the shaft ends closer to the motors. The operating/forcing protocols were programmed using LabVIEW. The turbulent velocity field generated by the active grid was analyzed using the stereoscopic particle image velocimetry (Stereo PIV) technique. The field of view was a 10" (2.5 M) square centered at a distance of 40" (x/M = 10) from the active grid. A total of 1500 flow field images were captured at a sampling rate of 60Hz and were time averaged to obtain the mean flow and velocity fluctuations. The turbulence intensity was measured as

$$Ti = 100\sqrt{\frac{\sigma^2(u)+\sigma^2(v)+\sigma^2(w)}{3(U_\infty{}^2+V_\infty{}^2+W_\infty{}^2)}} \qquad (1)$$

Where U_∞, V_∞ and W_∞ are the time averaged velocity components along the three coordinate directions and u, v and w are the corresponding instantaneous velocity fluctuations. $\sigma^2(u)$ Represents the variance of the respective fluctuating velocity component. A convergence study that monitored the time averaged velocity and the root mean square velocity fluctuation was performed to ensure that the statistics remained stationary with respect to sampling time. The non dimensional downstream distance of 10 chosen was found to be sufficient to restrict the anisotropy ratios to values below < 10%.

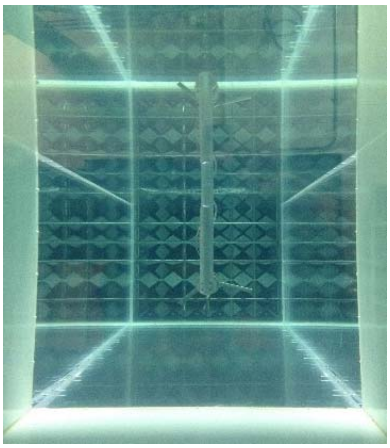

FIGURE 1. ACTIVE GRID TURBULENCE GENERATOR AT LEHIGH (VIEW FROM ACRYLIC WINDOW IN EXIT PLENUM)

An SG6043 hydrofoil cross sectioned wing model, with a chord length of 0.1397m and a span of 0.5588m, was used for the experiments. The model was suspended into the water tunnel test section from a support structure on top of the test section (see

figure 2) and was placed at a downstream distance of 48" (12*M*) from the grid. The lift and drag forces acting on the wing are measured using a 3 axis FUTEK load cell attached to the top end of the wing. The measured lift and drag loads were used to determine the lift and drag coefficients defined as:

$$C_L = \frac{L}{0.5\rho_\infty U_\infty^2 S}, C_D = \frac{D}{0.5\rho_\infty U_\infty^2 S} \quad (2)$$

where L and D are the lift and drag loads, C_L and C_D are the corresponding non dimensional lift and drag coefficients, ρ_∞ is the freestream density, U_∞ is the freestream velocity and S is the planform area. All experiments were performed at a chord based Reynolds number of 1.1×10^5 and Froude number of 0.33.

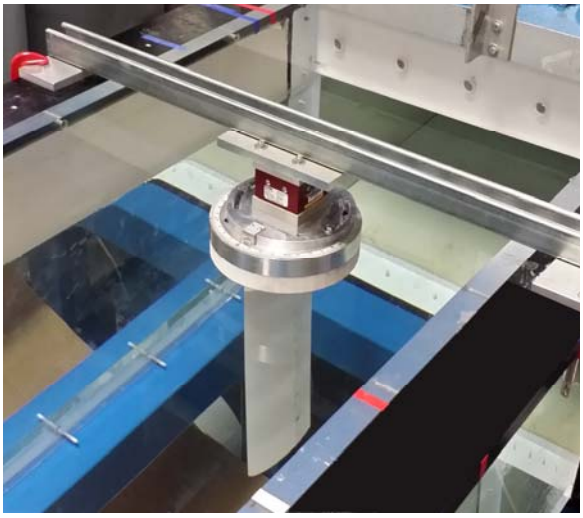

FIGURE 2. HYDROFOIL SETUP

RESULTS

Preliminary testing of the active grid was performed at a freestream velocity of 0.2 m/s. Figure 3 presents the turbulence intensities obtained using the random protocols for two different grid configurations; the 10 shaft configuration (both horizontal and vertical shafts) and the 5 shaft configuration (only horizontal shafts). With all 10 shafts, turbulence intensities as high as ~20% was obtained using both the random protocols. Clearly, the measured intensities seem to be a strong function of the solidity of the grid (number of shafts in this case). The intensities obtained with the 10 shaft configuration is consistently greater than that obtained using the five shaft configuration. Also, the rotation rate of the shafts and the employed forcing protocol have an effect on the obtained values of turbulence intensities.

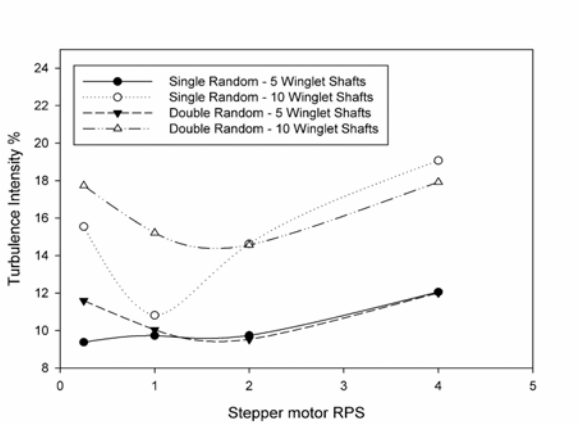

FIGURE 3. TURBULENCE INTENSITIES OBTANED WITH THE GRID

For the purposes of testing the effect of free stream turbulence on the performance of the SG6043 hydrofoil, turbulence was assessed at a higher free stream flow velocity of 0.8 m/s. A 2Hz double random protocol resulting in a turbulence intensity of 8% was used as the turbulent free stream condition. A low turbulence intensity case Ti = 1% (without the active grid) was also used as the laminar free stream case (base case). Coefficients of lift and drag were measured as a function of the angle of attack and are plotted in figure 4.

At lower angles, 0^o and 5^o the coefficient of lift observed in the turbulent flow is almost similar to the coefficient of lift observed in the laminar flow case. As the angle of attack increases, the lift force experienced by the hydrofoil becomes considerably more in the turbulent free stream case. The lift coefficient observed at an angle of attack of 10^o is ~ 6% more with a turbulent free stream and the percentage increase remains within this range until an angle of attack of 20^o. Beyond this angle the increase in measured lift forces goes beyond 20% reaching 22% at an angle of attack of 25^o. A very noticeable effect of free stream turbulence is its influence on flow separation and stalling of the hydrofoil. From the presented coefficient of lift measurements it can be identified that stalling, in case of the laminar free stream occurs beyond an angle of attack of 20^o, whereas in case of the turbulent free stream stall occurs beyond a slightly higher angle of attack of 22.5^o. In the post stall region, the decrease in lift observed in a turbulent flow is lower when compared to the laminar flow case. With a 2.5^o increase in angle of attack beyond stall, the lift coefficient in a turbulent free stream drops by 0.5%, whereas the same in a laminar freestream drops by 2%.

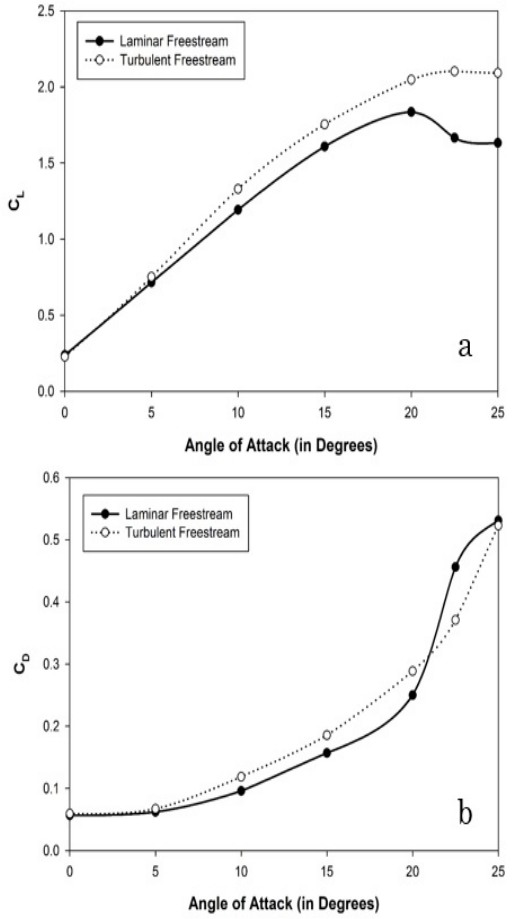

FIGURE 4. VARIATIONOF (a) C_L (b) C_D WITH ANGLE OF ATTACK

The drag coefficient gradually increases with angle of attack for both the cases. In the case with the turbulent free stream, the measured drag force is higher compared to the laminar free stream case, with the maximum percentage increase being 18% at an angle of attack of 10°. However, the trend is inversed beyond an angle of 20°. With stall occurring in the case of the laminar free stream the drag coefficient undergoes an 82% increase going from an angle of attack of 20° to 22.5°. In the case of the turbulent free stream the increase in drag observed with stall is approximately half of that observed with laminar free stream case i.e. ~40%. In order to better assess the hydrodynamic performance of the hydrofoil, its lift to drag ratio is presented in figure 5. For angles ranging from 0° to 20°, the lift/drag ratio observed in the turbulent free stream in lower than the values observed in the laminar free stream (the difference being less than 10%) hinting towards a slightly compromised performance. For angles greater than 20°, the previously discussed increase in lift and decrease in drag in the post stall regime considerably increase the measured Lift/Drag ratio in the turbulent free stream, 50% at 22.5° and 32% at 25°, increasing its performance.

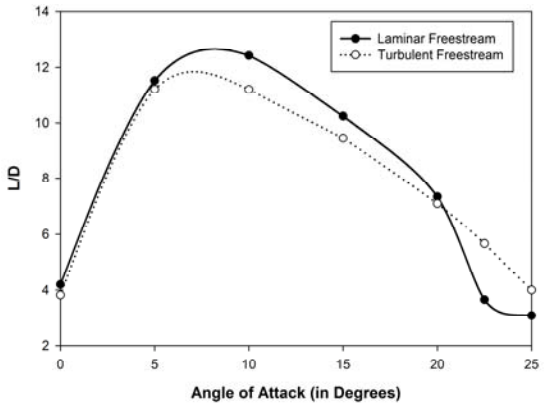

FIGURE 5. VARIATION OF L/D WITH ANGLE OF ATTACK

CONCLUSION

An active grid type dynamic turbulence generator developed for a horizontal test section water tunnel facility was used to perform the preliminary testing of the effect of FST on the loads experienced by a SG6043 hydrofoil. FST was shown to influence the stall angle and hence separation of flow around the hydrofoil. Stall occurred at an angle of 20° in the laminar freestream, whereas was postponed to 22.5° in the turbulent freestream. The hydrofoil experienced considerably higher lift forces in a turbulent flow with the increase being as significant as 20% in the post stall regime. A higher drag was experienced in turbulent free stream conditions until an angle of 20°. Beyond the stall angle the drag and rate of increase in drag observed in the laminar free stream was higher than the turbulent free stream. Based on the L/D ratios measured under the tested conditions it can be concluded that turbulence causes a decrease in performance while operating in the pre stall regime, however augments performance of the hydrofoil in the post stall regime.

REFERENCES

[1]. Mycek, P., et al., 2014, "Experimental study of the turbulence intensity effects on marine current turbines behaviour. Part I: One single turbine". Renewable Energy. **66**: pp. 729-746.
[2]. Zdravkovich, M., 1997, "Flow around Circular Cylinders; Vol. I Fundamentals". Journal of Fluid Mechanics. **350**(1): pp. 377-378.
[3]. Bearman, P.W. and T. Morel, 1983, "Effect of free stream turbulence on the flow around bluff

bodies". Progress in Aerospace Sciences. **20**(2–3): pp. 97-123.
[4]. Gad-el-Hak, M. and C.-M. Ho, 1986, "Unsteady vortical flow around three-dimensional lifting surfaces". AIAA journal. **24**(5): pp. 713-721.
[5]. Thompson, B. and J. Whitelaw, 1988, "Flow-around airfoils with blunt, round, and sharp trailing edges". Journal of aircraft. **25**(4): pp. 334-342.
[6]. Gad-el-Hak, M. and S. Corrsin, 1974, "Measurements of the nearly isotropic turbulence behind a uniform jet grid". Journal of Fluid Mechanics. **62**(01): pp. 115-143.
[7]. Makita, H., 1991, "Realization of a large-scale turbulence field in a small wind tunnel". Fluid Dynamics Research. **8**: pp. 53-64.
[8]. Makita, H. and S. Miyamoto. *Generation of high intensity turbulence and control of its structure in a low speed wind tunnel*. in *Proceedings of 2nd Asian congress on fluid mechanics*. 1983.
[9]. Larssen, J.V., *Large scale homogeneous turbulence and interactions with a flat-plate cascade*, in *Aerospace Engineering*. 2005, Virginia Tech.
[10]. Mydlarski, L. and Z. Warhaft, 1996, "On the onset of high-Reynolds-number grid-generated wind tunnel turbulence". Journal of Fluid Mechanics. **320**: pp. 331-368.
[11]. Poorte, R.E.G. and A. Biesheuvel, 2002, "Experiments on the motion of gas bubbles in turbulence generated by an active grid". Journal of Fluid Mechanics. **461**: pp. 127-154.
[12]. Mukherji, S.S., et al., 2011, "Numerical investigation and evaluation of optimum hydrodynamic performance of a horizontal axis hydrokinetic turbine". Journal of renewable and sustainable energy. **3**(6): pp. 063105.
[13]. Kolekar, N. and A. Banerjee, 2015, "Performance characterization and placement of a marine hydrokinetic turbine in a tidal channel under boundary proximity and blockage effects". Applied Energy. **148**: pp. 121-133.
[14]. Maldonado, V., et al., 2015, "The role of free stream turbulence with large integral scale on the aerodynamic performance of an experimental low Reynolds number S809 wind turbine blade". Journal of Wind Engineering and Industrial Aerodynamics. **142**: pp. 246-257.